Journal of Information Display
Vol. 12, No. 4, December 2011, 205–208

Taylor & Francis
Taylor & Francis Group

Integration of solution-processed polymer thin-film transistors for reflective liquid crystal applications

Sung-Jin Kim[a]*, Min-Hoi Kim[b], Min Chul Suh[c], Yeon-Gon Mo[d], Seung Wook Chang[d] and Sin-Doo Lee[b]

[a]*College of Electrical and Computer Engineering, Chungbuk National University, Cheongju 361-763, South Korea;*
[b]*School of Electrical Engineering, Seoul National University, Kwanak PO Box 34, Seoul 151-600, South Korea;*
[c]*Department of Information Display, Kyung Hee University, Dongdaemoon-Gu, Seoul 130-701, South Korea;*
[d]*R&D Center, Samsung Mobile Display, Co., Ltd., Gyeonggi-do 449-902, South Korea*

(*Received 12 July 2011; Revised 14 August 2011; Accepted 23 August 2011*)

Herein, the integration of solution-processed polymer thin-film transistors (TFTs) that were fabricated using selective wettability through ultraviolet (UV) exposure into a reflective liquid crystal display is demonstrated. From the experimental results of energy-dispersive spectroscopy, the composition of carbon and fluorine enhancing the hydrophobicity in the polymer chains was found to play a critical role in the wetting selectivity upon UV exposure. The polymer TFTs fabricated through the wettability-patterning process exhibited long-term stability and reliability. This wetting-selectivity-based patterning technique will be useful for constructing different types of solution-processed electronic and optoelectronic devices.

Keywords: wetting selectivity; solution-processed; hydrophobic; polymer TFT; liquid crystal display

1. Introduction

Organic thin-film transistors (OTFTs) have attracted much attention of late for use as driving elements in flat-panel displays [1–3], complementary circuits [4,5], radio frequency identification tags [6,7], and chemical or biological sensors [8–10]. In contrast to the conventional inorganic amorphous silicon thin-film transistors (TFTs) that require expensive and complicated fabricating steps at a high temperature [11], vapor- and solution-deposited OTFTs on plastic substrates allow for relatively easy fabrication due to their chemical tailoring capability [12,13]. In particular, solution-processed polymer TFTs provide new opportunities to produce low-cost and large-area device applications because the electrodes and active layers in the polymer TFTs can be processed at a low temperature.

With the increasing demand for inexpensive, lightweight, flexible devices, solution-processed polymer TFTs have served as essential elements for driving organic displays. For example, a high-mobility conjugated polymer TFT was demonstrated to drive a similar-sized polymer light-emitting diode [1]. Although significant progress has been made in improving the performance of the solution-processed polymer TFTs for the backplane, the development of a reliable patterning technique and a method of integrating individual elements into an array has so far been limited.

In this work, an integration scheme of solution-processed polymer TFTs into a reflective liquid crystal display (LCD) is demonstrated by utilizing the full benefits of wettability patterning, a concept that had been reported earlier [14,15]. The control of the wetting selectivity by ultraviolet (UV) light is capable of defining high-resolution patterns of a solution-based semiconducting polymer.

2. Control of the wetting selectivity for active-layer patterns

Although a direct laser ablation method is a solvent-free process of achieving high-resolution patterns in large-area devices [16,17], it may involve some unexpected damages and/or changes in the chemical composition of an organic semiconducting layer during laser irradiation and may result in a parasitic leakage current in the fabricated OTFTs. In contrast, for solution-based semiconducting polymers, the wettability-patterning approach concerns only the selective ablation of a hydrophobic layer without directly patterning the semiconducting polymer layer for defining an active channel, as shown in Figure 1. In this case, the key concept is to generate selective wettability on a substrate so that the patterns of a soluble semiconducting polymer will be easily produced through simple coating in a large area. As shown in Figure 1, the fluorine-based hydrophobic-polymer layer CYTOP (Asahi Glass Co.,

*Corresponding author. Email: ksj@cbnu.ac.kr

ISSN 1598-0316 print/ISSN 2158-1606 online

http://dx.doi.org/10.1080/15980316.2011.621319
http://www.tandfonline.com

Ltd.) and TDUR-P015 (Tokyo Ohka Kogyo Co., Ltd.), a photoabsorption buffer layer below CYTOP, were simultaneously laser-ablated with 248 nm UV light through a quartz photomask. As the laser intensity increased, the photoabsorption layer started to thermally diffuse and eject small modules. Then the CYTOP layer itself became transiently hot, and a nanometer-scale hydrophobic-polymer-surface explosion was observed [18–20]. Through the simple coating of a solution of a semiconducting polymer, poly(9-9-dioctyfluorene-co-bithiophene) (F8T2), in xylene in 1 wt% onto the substrate, active-layer patterns of F8T2 were spontaneously formed according to the resultant selective wettability.

Next, how the wetting selectivity of the substrate surface is affected by the morphological properties and the composition of the substrate surface upon UV exposure shall be explained. Figure 2 shows the scanning electron microscopic (SEM) images, the contact angles (θ_{CA}), and the composition results obtained from energy-dispersive spectroscopy (EDS). As shown in Figure 2(a), the substrate surface was hydrophobic ($\theta_{CA} \approx 98.7°$) before UV exposure. At the UV intensity of 450 mW/cm^2, the surface became hydrophilic ($\theta_{CA} \approx 6.2°$), revealing that both the CYTOP and TDUR-P015 layers were completely removed, as shown in Figure 2(b). The hydrophilic nature can be understood from the EDS composition results in Figure 2(c), which shows the reduction of carbon and fluorine and the increase of oxygen with the increasing UV intensity. In other words, the hydrophobicity resulting from the carbon and fluorine in the CYTOP and TDUR-P015 layers decreased with the increasing UV intensity. At the UV intensity of 450 mW/cm^2, the substrate surface was mostly composed of oxygen and became essentially hydrophilic.

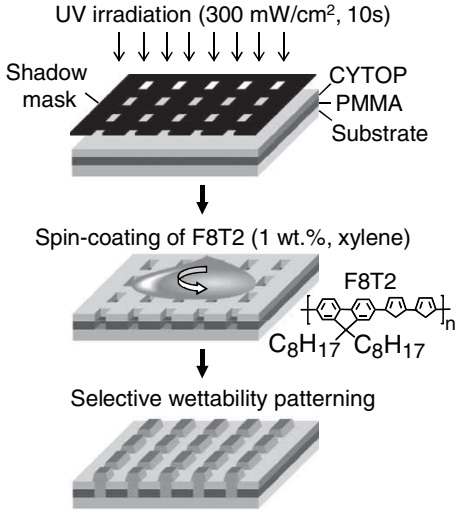

Figure 1. Schematic diagram of the patterning process based on the wetting selectivity.

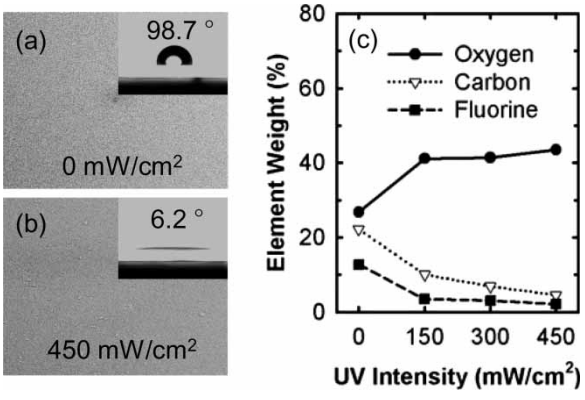

Figure 2. SEM images of the UV-irradiated substrate surfaces. The UV intensities that were used were (a) 0 mW/cm^2 and (b) 450 mW/cm^2. The inserts in (a) and (b) represent the contact angles. (c) Element weights of oxygen, carbon, and fluorine as a function of the UV intensity on the irradiated regions.

3. Fabrication of a polymer TFT array

Based on the selective wettability of the substrate surface described above, the integration of the polymer TFTs into an array for use as a backplane for display applications was demonstrated. The F8T2 patterns were used for constructing 30 × 30 polymer TFTs in an array format. A top view of the polymer TFT array (left) together with a schematic representation of one polymer TFT (right) is shown in

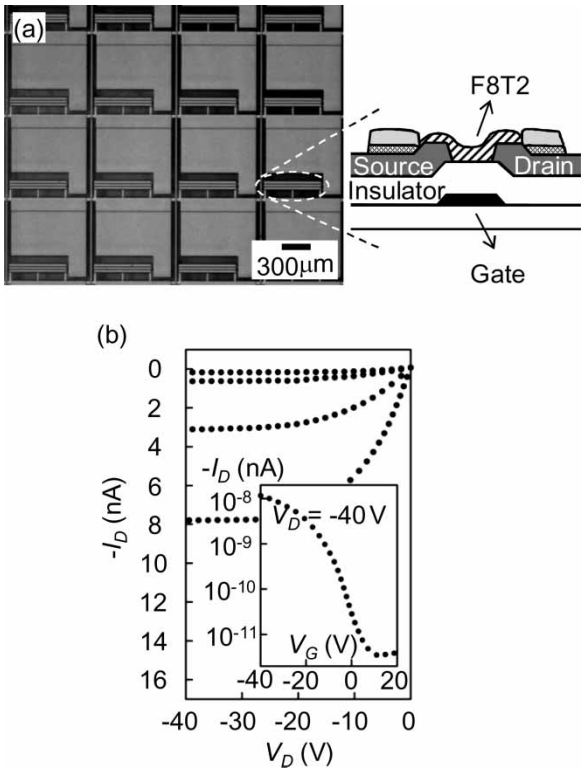

Figure 3. (a) Optical micrograph of an array of polymer TFTs integrated for use as the backplane of a reflective LCD (left) together with a schematic representation of one polymer TFT (right) and (b) the electrical characteristics of the polymer TFT.

Figure 3(a). In such a bottom-gate TFT architecture for a pixel TFT, the gate electrode was made of 100-nm-thick MoW, the gate insulator was made of 200-nm-thick SiO_2, and the drain and source electrodes were made of 100-nm-thick MoW. The electrodes and insulator layers were patterned via standard photolithography. The TFT channel length (L) and width (W) were 20 and 1800 μm, respectively.

Figure 3(b) shows the transfer and output characteristics of the polymer TFT. The drain current (I_D) as a function of the drain voltage (V_D) was measured for the several gate voltages (V_G) of 0, −10, −20, −30, and −40 V. From the transfer characteristics, an on–off current ratio larger than 10^3 was obtained. The results are the typical features of a field effect transistor in the linear and saturated regimes, as reported previously [14]. No considerable variations in the electrical performance among the polymer TFTs were observed. This is very important to maintain the uniformity throughout a display panel for large-area applications. It was noted that due to the large value of W/L and the issues associated with the interface between a metal layer (MoW) and an organic semiconductor (F8T2), the drain current of the polymer TFT ($\sim 10^{-9}$ A) was somewhat limited. This can be improved either by surface treatment, such as that with self-assembled monolayers on an insulator layer [21,22], or by the proper molecular ordering of the semiconducting polymers [23,24].

4. Construction of a reflective LCD with polymer TFTs

A prototype of a reflective LCD was constructed, which was operated with the polymer TFTs. The cross-section of one pixel composed of one polymer TFT and an liquid crystal (LC) layer is shown in Figure 4(a). The LC layer was prepared on the polymer TFT backplane, and the thickness of the LC layer was maintained using 5-μm-thick glass spacers. The LC that was used was MJ96758 (E. Merck) with a negative dielectric anisotropy (−4.9), and the alignment layer that was used was LGC-M1 (LG Cable, Ltd.), which vertically aligned the LC molecules through the illumination of UV light at 2.0 mW for 2 min. Indium tin oxide was used for the transparent electrode, and the MoW electrode served as a reflector. A quarter waveplate and a polarizer were placed in the front of the LCD panel for operation in the normally black mode.

The scan and data waveforms that were used for driving the 30 × 30 polymer TFTs are shown in Figure 4(b), and the frame rate was 30 Hz. The polymer TFT in each pixel acted as a switch to store the voltage on the pixel electrode. The addressing scheme that was used was accomplished by driving the rows (scan lines) one at a time, biasing the TFT gates low, and loading the data into the pixels from the column (data) lines. The image data were loaded when the TFT gates were turned on through the application of a voltage to a single row, and the data were then transferred to the

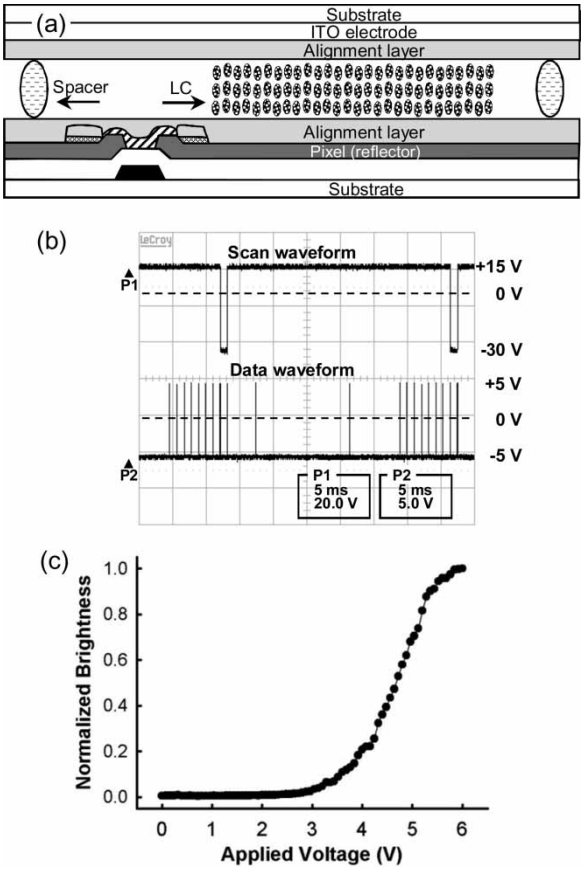

Figure 4. (a) Cross-section of one pixel composed of one TFT and an LC layer. (b) The scan and data waveforms that were used for driving 30 × 30 polymer TFTs in an array. The frame rate was 30 Hz. (c) The normalized brightness of the reflective LC cell as a function of the applied voltage.

pixels from the column (data) lines. Depending on the contrast (either black or white) of the pixel in the image, V_{data} of −5 or +5 V were, respectively, applied in the odd frame ($V_{com} = +5$ V) and V_{data} of +5 or −5 V, respectively, in the even frame ($V_{com} = -5$ V), as shown in Figure 4(b). The gate lines were driven at $V_G = -30$ V for the selection time and at $V_G = +15$ V for the holding time. Figure 4(c) shows the normalized brightness of the reflective LC cell as a function of the applied voltage. The electro optic (EO) brightness started to appear at the threshold voltage of about 3.4 V and it started to saturate above 6 V. Figure 5(a) shows the microscopic textures of a part of the pixel arrays for the different applied voltages of 0, 3.4, 4.9, and 5.8 V, giving the analog gray scale capability. In Figure 5(b), an image of 'SNU-MIPD-LAB' is displayed in the reflective LCD driven with the 30 × 30 polymer TFTs fabricated via selective wettability patterning. Although the image quality in the reflective LCD seems not to be high, no image degradation was observed over a few years under ambient conditions. This indicates that the array of the 30 × 30 polymer TFTs that were fabricated using selective wettability indeed possesses long-term stability and reliability.

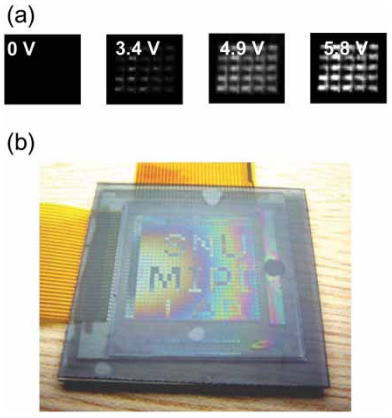

Figure 5. (a) Microscopic textures of a part of the pixel arrays for the different applied voltages of 0, 3.4, 4.9, and 5.8 V. (b) Image of 'SNU-MIPD-LAB' displayed in the reflective LCD driven with 30 × 30 polymer TFTs fabricated via selective wettability patterning.

5. Concluding remarks

A viable method of integrating solution-processed polymer TFTs into an array based on selective wettability was developed through UV exposure. The long-term stability and the reliability of the polymer TFTs were demonstrated in a reflective LCD, where the polymer TFTs were used as driving elements for displaying images. No image degradation in the reflective LCD was observed for a few years under ambient conditions. The wetting-selectivity-based patterning technique presented herein will be useful for constructing different types of solution-processed electronic and optoelectronic devices.

Acknowledgements

This work was supported in part by Samsung Mobile Display Co., Ltd. and by a research grant from Chungbuk National University 2010. Parts of this work were presented in IMID 2007.

References

[1] H. Sirringhaus, N. Tessler, and R.H. Friend, Science **280**, 1741 (1998).
[2] G.H. Gelinck, H.E. Huitema, E.V. Veenendall, E. Cantatore, L. Schrijnemakers, J.B.P.H.V.D. Putten, T.C.T. Genus, M. Beenhakkers, J.B. Giesbers, B.-H. Huisman, E.J. Meijer, E.M. Benito, F.J. Touwslager, A.W. Marsman, B.J.E.V. Rens, and D.M.De. Leeuw, Nat. Mater. **3**, 106 (2004).
[3] L.S. Zhou, A. Wanga, S.C. Wu, J. Sun, S. Park, and T.N. Jackson, Appl. Phys. Lett. **88**, 083502 (2006).
[4] H. Klauk, U. Zschieschang, J. Pflaum , and M. Halik, Nature **445**, 745 (2007).
[5] X.H. Zhang, W.J. Potscavage, S. Choi, and B. Kippelen, Appl. Phys. Lett. **94**, 043312 (2009).
[6] D. Voss, Nature **407**, 442 (2000).
[7] R. Rotzoll, S. Mohapatra, V. Olariu, R. Wenz, M. Grigas, K. Dimmler, O. Shchekin, and A. Dodabalapur, Appl. Phys. Lett. **88**, 123502 (2006).
[8] Z.-T. Zhu, J.T. Mason, R. Dieckmann, and G.G. Malliaras, Appl. Phys. Lett. **81**, 4643 (2002).
[9] L. Torsi, G.M. Farinola, F. Marinelli, M.C. Tanese, O.H. Omar, L. Valli, F. Babudri, F. Palmisano, P.G. Zambonin, and F. Naso, Nat. Mater. **7**, 412 (2008).
[10] L. Torsi, F. Marinelli, M.D. Angione, A. Dell'Aquila, N. Cioffi, E. De Giglio, and L. Sabbatini, Org. Electron. **10**, 233 (2009).
[11] M. Halik, H. Klauk, U. Zschieschang, G. Schmid, C. Dehm, M. Schutz, S. Maisch, F. Effenberger, M. Brunnbauer, and F. Stellacci, Nature **431**, 963 (2004).
[12] C.D. Dimitrakopoulos and P.R.L. Malenfant, Adv. Mater. **14**, 99 (2002).
[13] M.M. Ling and Z. Bao, Chem. Mater. **16**, 4824 (2004).
[14] S.-J. Kim, T. Ahn, M.C. Suh, C.-J. Yu, D.-W. Kim, and S.-D. Lee, Jpn. J. Appl. Phys. **44**, L1109 (2005).
[15] S.-J. Kim, J.-H. Bae, T. Ahn, M.C. Suh, S.W. Chang, Y.-G. Mo, H.-K. Chung, and S.-D. Lee, Proc. 7th Int'l Meeting on Information Display (IMID 2007), 152 (2007).
[16] H.M. Philips, D.L. Callahan, R. Sauerberey, G. Szabo, and Z. Bor, Appl. Phys. Lett. **58**, 2761 (1991).
[17] R. Srinivasan and B. Braren, Chem. Rev. **89**, 1303(1989).
[18] C.S. Dulcey, J.H. Georger, Jr, V. Krauthamer, D.A. Stenger, T.L. Fare, and J.M. Calvert, Science **252**, 551 (1991).
[19] D.D. Saperstein and L.J. Lin, Langmuir **6**, 1522 (1999).
[20] W.J. Leigh, Chem. Rev. **93**, 487 (1993).
[21] K.P. Pernstich, S. Haas, D. Oberhoff, C. Goldmann, D.J. Gundlach, B. Batlogg, A.N. Rashid, and G. Schitter, J. Appl. Phys. **96**, 6431 (2004).
[22] Y. Wu, P. Liu, B.S. Ong, T. Srikumar, N. Zhao, G. Botton, and S. Zhu, Appl. Phys. Lett. **86**, 142102 (2005).
[23] H.E. Katz, Z. Bao, and S.L. Gilat, Acc. Chem. Res. **34**, 359 (2001).
[24] H. Sirringhaus, P.J. Brown, R.H. Friend, M.M. Nielsen, K. Bechgaard, B.M.W. Langeveld-Voss, A.J.H. Spiering, R.A.J. Janssen, E.W. Meijer, P. Herwig, and R.M. De Leeuw, Nature **401**, 685 (1999).